Damage-Mitigating Control of a Reusable Rocket Engine

Asok Ray,* Xiaowen Dai,† Min-Kuang Wu,† and Marc Carpino‡
Pennsylvania State University, University Park, Pennsylvania 16802
and
Carl F. Lorenzo§
NASA Lewis Research Center, Cleveland, Ohio 44135

This article presents a control concept for damage prediction and damage mitigation in reusable rocket engines for enhancement of structural durability. The key idea here is to achieve high performance without overstraining the mechanical structures so that 1) the functional lives of critical components are increased, resulting in enhanced safety, operational reliability, and availability; and 2) the plant (i.e., the rocket engine) can be inexpensively maintained, and safely and efficiently driven under different operating conditions. To this effect, dynamics of fatigue damage have been modeled in the continuous-time setting instead of the conventional cycle-based approach, and an optimal control policy is formulated by constraining the accumulated damage and its time derivative. Efficacy of the proposed damage mitigation concept is evaluated for life extension of the turbine blades of a bipropellant rocket engine via simulation experiments. The simulation results demonstrate the potential of increasing the structural durability of reusable rocket engines with no significant loss of performance.

I. Introduction

A MAJOR goal in the control of a reusable rocket engine is to achieve high performance with increased reliability, availability, component durability, and maintainability.[1-3] The specific requirements are 1) extension of the service life of the controlled process, 2) increase of the mean time between major maintenance actions, and 3) reduction of risk in the design of integrated control-structure-materials systems. Therefore, rocket engine control systems need to be synthesized by taking performance, mission objectives, service life, and maintenance and operational costs into consideration. The current state-of-the-art in control systems synthesis for complex mechanical systems focuses on improving dynamic performance and diagnostic capabilities under the constraints that often do not adequately represent the material properties of the critical plant components. The reason is that the traditional design is based upon the assumption of conventional materials with invariant characteristics. In view of high-performance requirements and availability of improved materials that may have significantly different damage characteristics relative to conventional materials, the lack of appropriate knowledge about the properties of these materials will lead to either of the following: less than achievable performance due to overly conservative design, or overstraining of the structure leading to unexpected failures and drastic reduction of the useful life span.

Specifically, reusable rocket engines present a significantly different problem in contrast to expendable propulsion systems that are designed on the basis of minimization of weight and acquisition cost under the constraint of specified system reliability. In reusable rocket engines, multiple start-stop cycles cause large thermal strains; steady-state stresses generate inelastic strains; and dynamic loads induce high cyclic strains leading to fatigue failures. For example, the original design

goal of the Space Shuttle main engine was specified for 55 flights before any major maintenance, but the current practice is to disassemble the engine after each flight for maintenance.[1] Another example is design modification of the F-18 aircraft as a result of conversion of the flight control system from analog to digital, which would lead to a significant change in the load spectrum on the airframe structure. In this case, a major goal of the vehicle control systems redesign should be to achieve a tradeoff between flight maneuverability and durability of the critical components.[4]

As the science and technology of materials continue to evolve, the design methodologies for damage-mitigating control must have the capability of easily incorporating an appropriate representation of material properties. This requires augmentation of the system-theoretic techniques for synthesis of decision and control laws with governing equations and inequality constraints that would model the mechanical properties of the materials for the purpose of damage representation and failure prognosis. The major challenge in this research is to characterize the damage generation process, and then utilize this information in a mathematical form for synthesizing algorithms of robust control, diagnostics, and risk assessment in complex mechanical systems.

II. Damage-Mitigating Control System

The damage-mitigating control system, also referred to as life extending control system,[1] is intended to function independently, or as an integral part of a hierarchically structured intelligent control system[5] for plant operations. Figure 1 shows
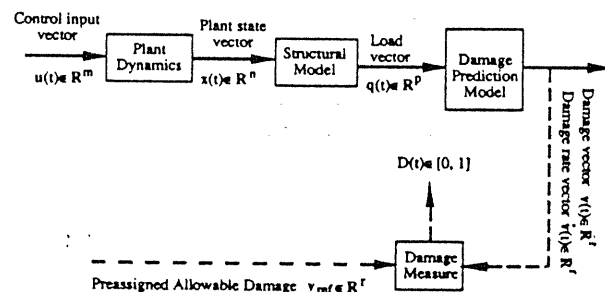
*Professor of Mechanical Engineering. Associate Fellow AIAA.
†Graduate Student, Mechanical Engineering Department.
‡Assistant Professor of Mechanical Engineering.
§Head, Systems Dynamics Branch, 21000 Brookpark Road.

Fig. 1 Damage prediction system.

a conceptual view of the damage prediction system which is an essential ingredient of the proposed damage-mitigating control system. The plant model is a finite-dimensional state-space representation of the system dynamics (e.g., thermal-hydraulic dynamics of the Space Shuttle main engine or propulsion and aerodynamics of an aircraft). The plant states are inputs to the structural model which, in turn, generates the necessary information for the damage model. The output of the structural model is the *load vector* which may consist of (time-dependent) variables such as stress, strain, and temperature at the critical point(s) of the structure. The damage model is a continuous-time (instead of being a cycle-based) representation of life prediction such that it can be incorporated within the control system model in the state-variable setting. The objective is to include, within the control system, the effects of damage rate and accumulated damage at the critical point(s) of the structure which may be subjected to time-dependent load. The damage state vector $v(t)$ could indicate the level of microcracking, macroscopic crack length, wear, creep, density of slip bands, etc., at one or more critical points, and its time derivative $\dot{v}(t)$ indicates how the instantaneous load is affecting the structural components. The overall damage $D(t)$ is a scalar measure of the combined damage at the critical point(s) resulting from (possibly) different effects (e.g., fatigue and creep) relative to the preassigned allowable level v_{ref} of the damage vector. Although $D(t)$ may not directly enter the feedback or feedforward control of the plant, it can provide useful information for intelligent decision-making such as damage prognosis and risk analysis.[3,5]

The plant and damage dynamics in Fig. 1 are modeled by nonlinear (and possibly time-varying) differential equations which must satisfy the local Lipschitz condition[6] within the domain of the plant operating range. The structural model in Fig. 1 consists of solutions of structural dynamic (typically finite element) equations representing the (mechanical and thermal) load conditions. A general structure of the plant and damage dynamics and their constraints is represented in the deterministic setting as follows:

Task period: Starting time t_0 to final time t_f

Plant dynamics

$$\dot{x} \equiv \frac{dx}{dt} = f[x(t), u(t), t], \qquad x(t_0) = x_0 \qquad (1)$$

Damage dynamics

$$\dot{v} \equiv \frac{dv}{dt} = h[v(t), q(x, t), t], \quad v(t_0) = v_0, \quad h \geq 0 \quad \forall t \quad (2)$$

Damage measure

$$D(t) = \xi[v(t), v_{ref}] \qquad \text{and} \qquad D(t) \in [0, 1] \qquad (3)$$

Damage rate tolerance

$$0 \leq h[v(t), q(x, t), t] < \beta(t) \qquad \forall t \in [t_0, t_f] \qquad (4)$$

Accumulated damage tolerance

$$[v(t_f) - v(t_0)] < \Gamma \qquad (5)$$

where

$x \quad \in R^n$ is the plant state vector
$u \quad \in R^m$ is the control input vector
$v \quad \in R^r$ is the damage state vector
$v_{ref} \in R^r$ is the preassigned limit for the damage state vector
$\beta \quad \in R^r$ and $\Gamma \in R^r$ are specified tolerances for the damage rate and accumulated damage, respectively
$q \quad \in R^p$ is the load vector
$D \quad \in [0, 1]$ is a scalar measure of the accumulated damage

The state-variable representation of the fatigue damage model in Eq. (2) allows the instantaneous damage rate $\dot{v}(t)$ to be dependent on the current level $v(t)$ of accumulated damage. The physical interpretation of the above statement is that a given test specimen or a plant component, under identical stress-strain hysteresis, shall have different damage rates for different initial damage. For example, if the initial crack length is 100 μm, the crack propagation rate will be different from that for a crack length of 20 μm under identical stress excursions.

The vector differential Eqs. (1) and (2) become stochastic if the randomness of plant and material parameters is included in the models, or if the plant is excited by discrete events occurring at random instants of time.[7] The stochastic aspect of damage-mitigating control is a subject of future research, and is not addressed in this article.

The open loop control policy is obtained via nonlinear programming[8] in N steps representing the period from the initial time t_0 to the final time t_f. The objective is to minimize a specified cost functional J (which includes plant state, damage rate, and control input vectors) without violating the prescribed bounds of the damage rate and the accumulated damage. The cost functional J is to be chosen in an appropriate form, representing a tradeoff between the system performance and the predicted damage. The design variables to be identified are the control inputs u_k, $k = 0, 1, 2, \ldots, N - 1$, and the goal is to search for an optimal control sequence $\{u_k\}$. The constraints on damage rate and accumulated damage need to be appropriately chosen by taking the mission objectives, the time interval between maintenance actions, service life, and allowable risk into consideration. The initial damage is important due to its significant effects on the dynamics of damage accumulation. The optimization problem is then formulated as follows:

Minimize:

$$J = \sum_{k=0}^{N-1} J_k(\tilde{x}_{k+1}, \dot{v}_k, \bar{u}_k) \qquad (6)$$

Subject to:

$$0 \leq h[v_k, q(x_k), k] < \beta(k) \qquad \text{and} \qquad (v_N - v_0) < \Gamma$$
$$\text{for } k = 1, 2, 3, \ldots, N \qquad (7)$$

where $\tilde{x}_k = x_k - x_{ss}$ and $\bar{u}_k = u_k - u_{ss}$ are deviations of the plant state vector and the control input vector from the respective final steady-state values of x_{ss} and u_{ss}; and $\beta(k) \in R^r$ and $\Gamma \in R^r$ are bounds on the damage rate and accumulated damage, respectively. Further details of the open loop control synthesis are reported by Ray et al.[3] and Wu.[9]

III.   Modeling of Damage Dynamics

Damage of mechanical structures is usually a result of fatigue, creep, corrosion, and their combinations. The prime focus in this research is the representation of fatigue damage in the continuous-time setting. As discussed earlier, a time-dependent model of damage dynamics, having the structure of Eq. (2), is necessary for analysis and synthesis of the damage-mitigating control system. From this perspective, a dynamic model of fatigue damage has been formulated in the continuous-time setting. Although this damage model has a deterministic structure, it can be recast in the stochastic setting to include the effects of both unmodeled dynamics and parametric uncertainties.

Because of the wide ranges in mechanical properties of materials, extensive varieties of experiments have been conducted for fatigue analysis, and many models have been proposed for fatigue life prediction in aerospace and ground vehicles.[10-12] Each of these models expresses the damage dynamics

by an equation with the number of cycles N as the independent variable. In contrast, the damage dynamics in Eq. (2) are expressed as a vector differential equation with respect to time t as the independent variable. The advantages of this approach are that it allows the damage model to be incorporated within the constrained optimization problem, and that the damage accumulated between any two instants of time can be derived even if the stress-strain hysteresis loop is not closed. This concept is applicable to different models of damage dynamics such as those resulting from cyclic strain or crack propagation. To this effect, we propose to model the continuous-time dynamics of fatigue damage based on the following two approaches.

1) *Cyclic strain-life*: In this approach, the local stress-strain behavior is analyzed at certain critical points where failure is likely to occur. The local strain may be directly measured from a strain gauge, or computed via finite element analysis. The local stress is estimated from the cyclic stress-strain curve. A cycle-based approach is then used to estimate the fatigue damage from the strain-life curves at different levels of stress and strain in the load history. We propose to determine the damage accumulation within a cycle using the classical Palmgren-Miner rule, and subsequently modify it via the damage curve approach of Bolotin.[13]

2) *Linear elastic fracture mechanics (LEFM)*: The LEFM approach is built upon the concept of a physical measure of damage in terms of the crack length and the size of the plastic zone at the crack tip.[14] The accumulated damage is computed by integrating the crack growth rate over the number of cycles. This is based on the crack growth rate equation being approximated by an exponential function of stress intensity factor range of the component.[15] The component is assumed to fail when the crack reaches the critical length which, in turn, is determined from the fracture toughness of the component on the basis of experimental data.

A. Damage Modeling via Cyclic Strain-Life

The cyclic strain-life approach recognizes that the fatigue life is primarily controlled by the local strain at the critical point(s) of the component. The first goal is to model linear damage accumulation in the continuous-time setting. Referring to Fig. 2, let point O be the starting (reference) point of a reversal, let A and B be two consecutive points on the same rising reversal, and let N_A and N_B represent the total number of cycles to failure with constant load amplitudes, $OA/2$ and $OB/2$, respectively. Then, the half-cycle increment of linear damage δ between points A and B is defined as

$$\Delta\delta = \frac{1}{N_B} - \frac{1}{N_A} \qquad (8)$$

In Eq. (8), it is assumed that the damage occurs only on the rising reversal, i.e., if the stress is monotonically increasing, and no damage occurs during unloading, i.e., if the stress is monotonically decreasing. This assumption is consistent with the physical phenomena observed in the fatigue crack prop-
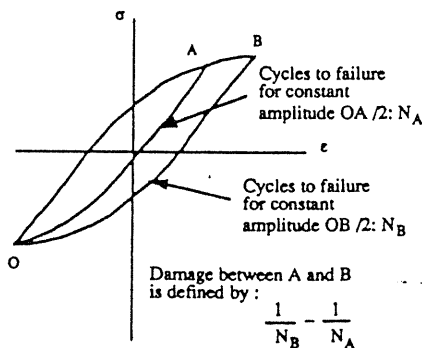
agation process. Replacing N_f by $1/\delta$, the strain life relationship[16] can be written as

$$\frac{|\varepsilon - \varepsilon_r|}{2} = \frac{\sigma_f' - \sigma_m}{E}\left(\frac{\delta}{2}\right)^{-b} + \varepsilon_f'\left(1 - \frac{\sigma_m}{\sigma_f'}\right)^{(c/b)}\left(\frac{\delta}{2}\right)^{-c} \qquad (9)$$

where b, c, σ_f', and ε_f' are material constants; σ_m is the mean stress; ε_r is the total strain corresponding to the reference stress σ_r at the starting point of a given reversal as determined from the rainflow cycle counting method; and $|\varepsilon - \varepsilon_r|/2$ is the strain amplitude between the current point and the reference point. The above equation does not provide a closed form solution for the predicted damage δ. The general approach to solve this problem is to separate Eq. (9) into two different modes. The first term on the right side is a modification of the Basquin equation and corresponds to the so called elastic damage δ_e. The second term on the right side of Eq. (9) is a modification of the Coffin-Manson equation and corresponds to the so called plastic damage δ_p. These two damages, δ_e and δ_p, can be derived separately in an explicit form. Generally speaking, for high-cycle fatigue, the elastic damage yields more accurate prediction than the plastic damage, and vice versa for low-cycle fatigue. Therefore, the linear damage δ should be obtained as a weighted average of δ_e and δ_p, where the weights depend on the relative accuracy of the elastic and plastic modes of damage computation under the current load condition.

To represent the damage equation in the format of Eq. (2), let point A approach point B as shown in Fig. 2. Then, the damage rates for both elastic and plastic modes can be computed via differentiation of δ_e and δ_p. Converting the strain amplitudes into stress amplitudes from the cyclic stress-strain curve, the elastic and plastic damage rates are given as

If $\sigma \geq \sigma_r$, then

$$\frac{d\delta_e}{dt} = 2\frac{d}{d\sigma}\left\{\left[\frac{\sigma - \sigma_r}{2(\sigma_f' - \sigma_m)}\right]^{-(1/b)}\right\} \times \frac{d\sigma}{dt}$$

$$\frac{d\delta_p}{dt} = 2\frac{d}{d\sigma}\left[\frac{1}{\varepsilon_f'}\left(\frac{\sigma - \sigma_r}{2K'}\right)^{(1/n')}\left(1 - \frac{\sigma_m}{\sigma_f'}\right)^{-(c/b)}\right]^{-c-1} \times \frac{d\sigma}{dt} \qquad (10)$$

else $d\delta_e/dt = 0$ and $d\delta_p/dt = 0$, where n' is the cyclic-strain hardening exponent and K' is the cyclic-strength coefficient; n' and K' are equal to b/c and $\sigma_f'/[(\varepsilon_f')^{b/c}]$, respectively. The damage rate $d\delta/dt$ is obtained as the weighted average of the elastic and plastic damage rates such that

$$\frac{d\delta}{dt} = w\frac{d\delta_e}{dt} + (1 - w)\frac{d\delta_p}{dt} \qquad (11)$$

where the weighting function w is selected as the ratio of the elastic strain amplitude and total strain amplitude. Equations (10) and (11) are then used to obtain the damage rate at any instant. The damage increment between two consecutive points t_k and t_{k+1} on the same reversal can be calculated by integrating the damage differential $d\delta$. Wu[9] has reported a close agreement of the damage model developed in Eqs. (10) and (11) with the commonly used damage model in Eq. (9). This agreement was established by using the experimental data[12] on fatigue damage of MANTEN steel for automotive axles.

The continuous-time damage model in Eqs. (10) and (11) is derived on the basis of linear damage accumulation following the Palmgren-Miner's rule. Although this concept of linear damage accumulation has been widely used due to its simplicity in computation, the cumulative damage behavior is actually nonlinear.[10,13] Experimental results show that, for varying amplitude loading, the accumulated damage is dependent on the order in which the load cycles are applied.

Fig. 2 Damage between two points on the same reversal.

This phenomenon is known as the sequence effect. Since the structural components of complex mechanical systems are subjected to loads of varying amplitude, the linear rule of damage accumulation which is commonly used for fatigue life assessment could lead to erroneous results due to this sequence effect. Therefore, a nonlinear damage rule needs to be established for accurate prediction of the damage rate and damage accumulation in the critical components.

B. Modeling of Nonlinear Cumulative Damage Using the Damage Curve Approach

The concept of a nonlinear damage curve to represent the damage was first conceived by Marco and Starkey.[17] No mathematical representation of damage curve was proposed at that time because the physical process of damage accumulation was not adequately understood. Manson and Halford[18] proposed the double linear rule primarily based on the damage curve approach for treating cumulative fatigue damage. In their article, an effort was made to mathematically represent the damage curve and approximate it by two piecewise line segments. The total fatigue life was then divided into two phases so that the linear damage rule can be applied in each phase of the life. A concept similar to the damage curve approach was proposed by Bolotin[13] with a mathematical representation which does not necessarily assess the damage on the basis of cycles, and is more appropriate for modeling in the continuous-time setting. Bolotin used the following analytical relationship between the nonlinear accumulated damage D and the linear damage δ:

$$D = (\delta)^\gamma \qquad (12)$$

In Eq. (12), the γ parameter describes the nonlinearity of the damage curve, and is usually assumed to be dependent solely on the stress amplitude level.[18] High-strength materials usually yield very large values of γ, especially under high-cycle fatigue. At the initial stage of the fatigue life, a large γ creates a very small damage, which could be out of the range of precision of the computer. This necessitates formulation of a computationally practical method of damage prediction. It follows from a crack propagation model such as the Paris model[19] that the crack growth rate is dependent not only on the stress amplitude, but also on the current crack length. Recognizing the fact that the crack itself is an index of accumulated damage, it is reasonable to assume the γ-parameter to be dependent on both stress amplitude σ_a and the current level of damage accumulation D, i.e., $\gamma = \gamma(\sigma_a, D)$. Therefore, we propose the following modification of Eq. (12):

$$D = (\delta)^{\gamma(\sigma_a, D)} \qquad (13)$$

where D and δ are the current states of nonlinear and linear damage accumulation, respectively. Although Eq. (13) has an implicit structure, it can be solved via a recursive relationship.

A detailed development of the nonlinear damage model in the continuous-time setting has been reported by Ray et al.[2] and Wu.[9] In this model, the accumulated damage at any point within a reversal can be obtained by solving the following nonlinear equations:

$$\gamma = \gamma(\sigma_a, D)$$
$$D = (\delta + \Delta\delta)^\gamma \qquad (14)$$

where δ is the linear damage at the reference point of a reversal and $\Delta\delta$ is the linear damage increment for the stress amplitude σ_a relative to the reference point. A recursive relationship has been developed[2,9] for solving the implicit Eqs. (14), where the numerical method operates on a set of discrete points in the load history.

C. γ-Parameter Fitting for the Nonlinear Damage Model

One major task in the above approach is to identify a mathematical representation for the γ parameter as a function of the stress amplitude and the current damage state. It requires knowledge of the physical process of damage accumulation which may be obtained from either experimental data or a combination of experimental data and analysis, and an appropriate definition of damage. The γ parameters are different, in general, for different materials and follow different structures of the governing equations. Furthermore, because the mechanisms attributed to the damage accumulation at various stages of fatigue life are different, no single approach apparently provides a sufficiently accurate prediction of damage throughout the fatigue life of a component. It is difficult, if not impossible, to construct a single structure for representation of γ. An alternative approach is to evaluate γ by interpolation. Once the damage is appropriately defined, and an analytical method for damage prediction is selected, the information needed for the nonlinear damage model can be generated via experimentation or analysis for a set of constant

Table 1 List of state variables, control inputs, and measured variables for plant control

State variables	
Combustor gas pressure	Combustor gas density
Combustor cooling tube wall temperature	Nozzle cooling tube wall temperature
Combustor coolant temperature	Nozzle coolant temperature
H_2 turbopump shaft speed	O_2 turbopump shaft speed
H_2 preburner oxidant flow valve position	O_2 preburner oxidant flow valve position
H_2 preburner gas pressure	O_2 preburner gas pressure
H_2 preburner gas density	O_2 preburner gas density
Mass flow rate of hydrogen into the H_2 preburner	Mass flow rate of hydrogen into the O_2 preburner
Mass flow rate of oxygen into the H_2 preburner	Mass flow rate of oxygen into the O_2 preburner
	Mass flow rate of oxygen into the combustor

Control inputs	
Oxidant flow command into H_2 preburner	Oxidant flow command into O_2 preburner

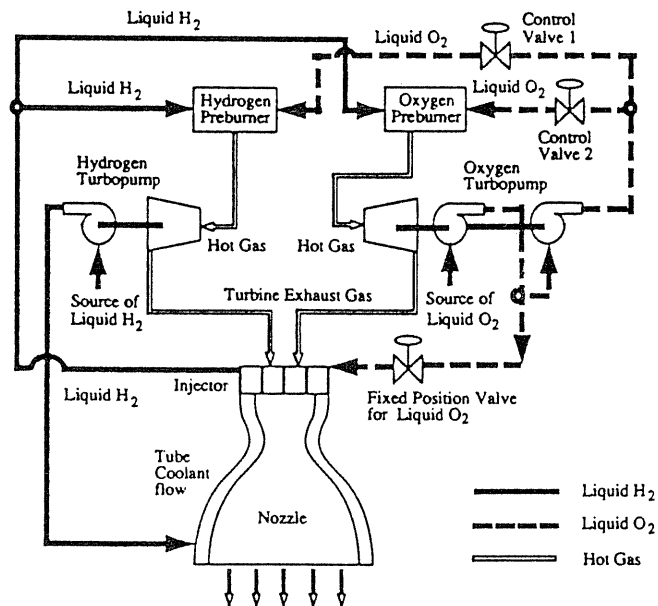| Measured variables for plant control	
Combustor chamber pressure	Ratio of O_2/H_2 flow rates

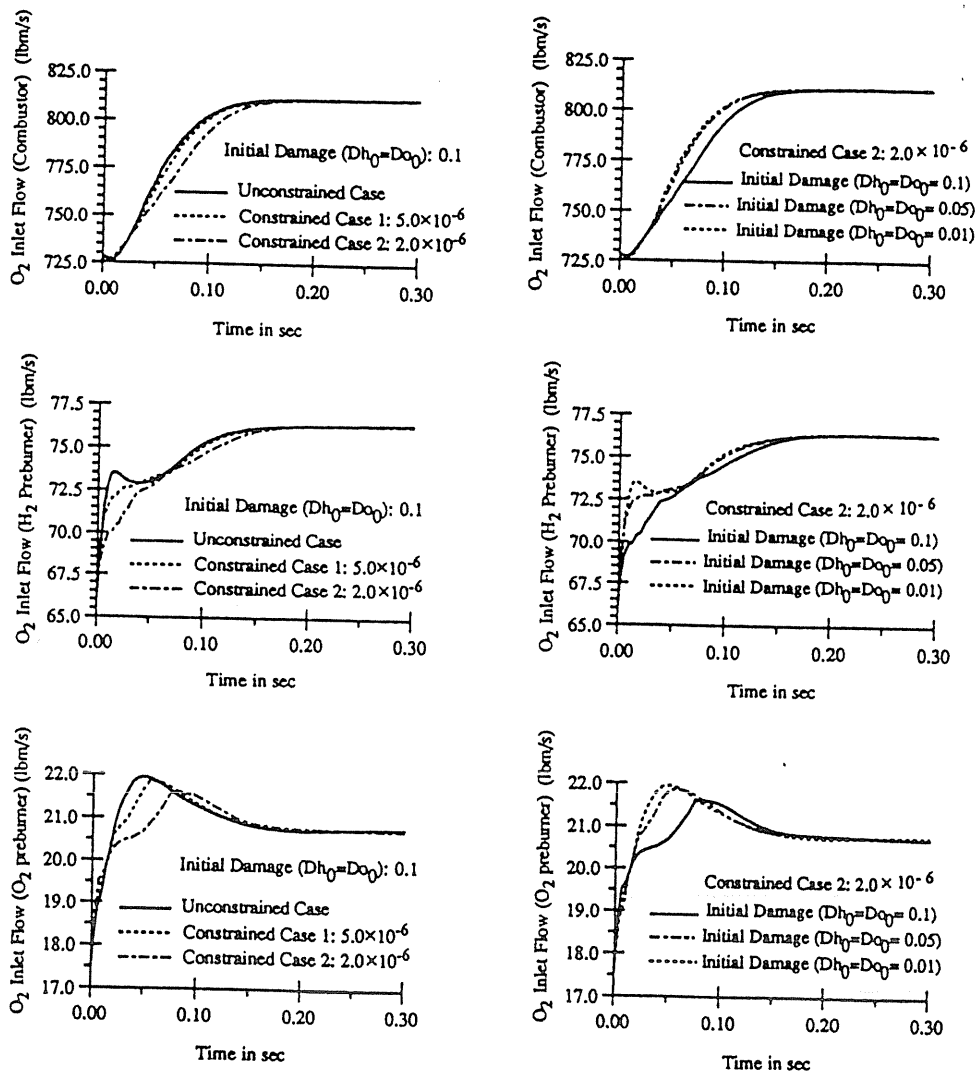Fig. 3 Schematic diagram of the bipropellant rocket engine.

Fig. 4 Transient responses of oxygen inlet flow to combustor and two preburners.

stress amplitudes. The values of γ are then computed by Eq. (13) for a given stress amplitude and the damage data ranging from the initial damage state D_0 to the failure condition at $D = 1$. The generated data, γ vs D, are then plotted for various amplitudes of stresses. These curves can be either fitted by nonlinear equations, if possible, or as linear piece-wise representations. Since it is not practical to perform experiments at infinitesimally small increments of stress amplitude, γ can be only experimentally evaluated at selected discrete levels of stress amplitude. The values of γ for other stress amplitudes can then be interpolated. Since the characteristics of γ may strongly depend on the type of the material, availability of pertinent experimental data for the correct material is essential for the damage-mitigating control synthesis. The γ parameter has been fitted based on the experimental data[20] for the material AISI 4340 steel. Details are reported by Ray et al.[2] and Wu.[9]

The nonlinear damage model in Eqs. (13) and (14) are valid for predicting *microscopic* cracks which occur within the crack initiation period defined in the usual sense of *macroscopic* cracks. For high-strength materials such as Ni-based super-alloys used in turbine blades that are subjected to high cycle fatigue, a significantly large part (e.g., as large as 98%), of the service life may be expended during this crack initiation period. Under these circumstances, the functional life of the stressed component is virtually exhausted even before the onset of the crack propagation phase because the damage rate can be extremely large after the appearance of a macrocrack. Therefore, the nonlinear fatigue damage model reported here represents almost the entire functional life of the critical com-

ponents under fatigue stress. It is important to note that the effects of thermomechanical fatigue (i.e., strain cycling at a high temperature and possibly accompanied by temperature cycling) are not included in the model of Eqs. (13) and (14). This is a subject of current research and the basic concepts are outlined by Ray et al.[2]

The control concept and the damage model presented above are potentially applicable to on-line monitoring of damage and prognosis of impending failures as discussed by Ray et al.[3] Conceptually, the damage model can be implemented in various ways for real-time execution. For example, if several critical points are considered for prediction of fatigue failure within a given component, then a single neural network can be trained over a selected operating range based on the results generated by the nonlinear damage model in Eqs. (13) and (14). Preliminary efforts in this direction have been reported by Troudet and Merrill.[21]

IV. Simulation Results and Discussion

The damage mitigation concept is applied, via simulation, to the open loop control of a reusable rocket propulsion engine such as one described by Sutton[22] and Duyar et al.[23] The plant model under control is a simplified representation of the dynamic characteristics of a bipropellant rocket engine as shown in Fig. 3. The two preburners serve as gas generators, and respectively drive the liquid hydrogen and liquid oxygen turbopumps. In this rocket engine, oxidant flow to each of the two preburners are independently controlled, while the oxidant flow valve into the main combustor chamber is held in a fixed position. The H_2 and O_2 turbopump speeds, and
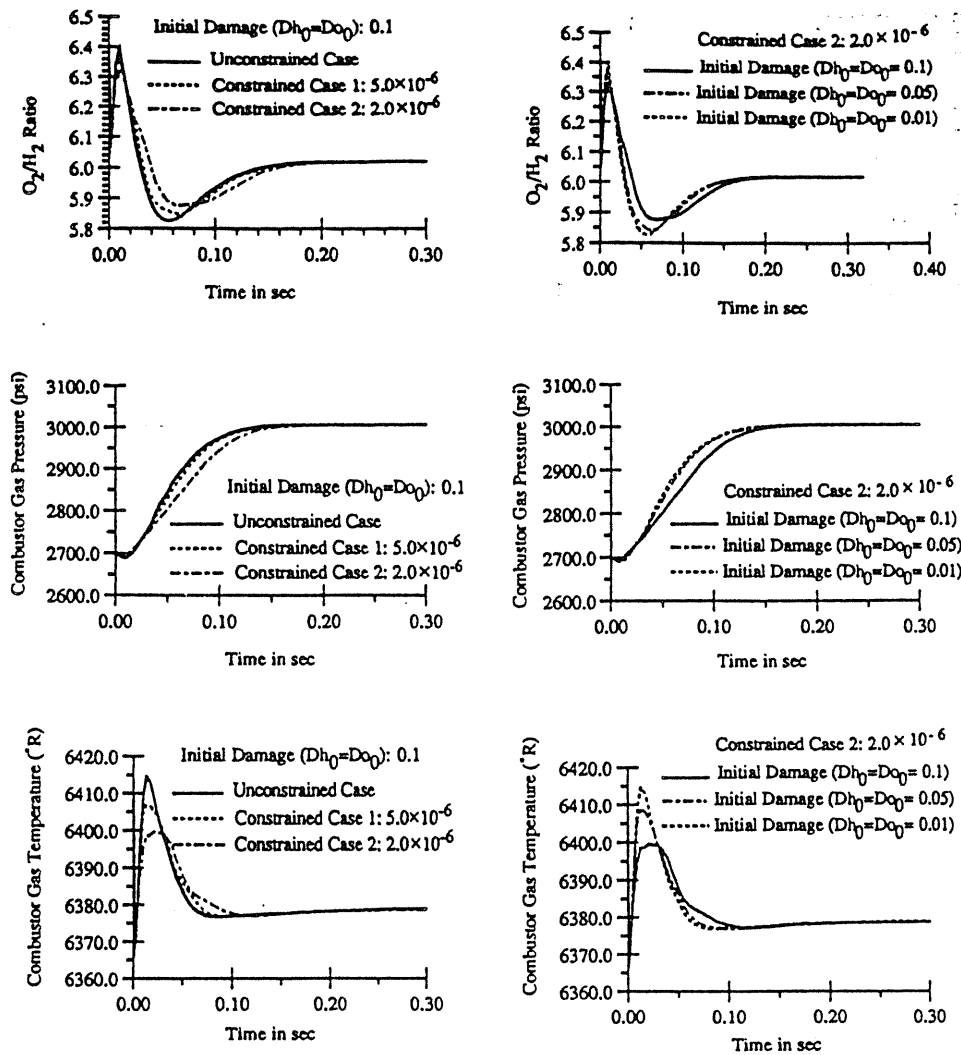
Fig. 5   Transient responses of oxygen/hydrogen ratio, combustor gas pressure, and temperature.

hence the propellant flow into the main combustor, are controlled by the respective preburner pressures. The nonlinear model of plant dynamics is derived in the state-space form based on the physical layout of the rocket engine in Fig. 3. Standard lumped parameter methods have been used to approximate the partial differential equations describing mass, momentum, and energy conservation by a set of first-order differential equations. In this model, the plant state vector consists of nineteen state variables, two control inputs, and two measured variables as listed in Table 1.

The structural model in Fig. 1 represents the cyclic mechanical stresses at the root of a typical blade in each of the H_2 and O_2 turbines, which are presumed to be the critical components in this study. The blade model for each of the two turbines is represented by a three-node beam model with 6 DOF at each node, while the first node at the root is kept fixed. The load on each blade model is assumed to consist of two components. The first component is due to the (time-dependent) drive torque which is derived as an output of the plant model. The second component is a dynamic term which represents the oscillatory load on the blade as it passes each stator. It is the second component that causes high cycle fatigue at the root of the blade, while the first component is largely responsible for the mean stress. The fatigue damage model formulated in Secs. II and III was used to generate the results in Figs. 4–7.

The purpose of this simulation study is to examine the dynamic performance and damage of the nominal plant when the two oxidant valves are manipulated to vary the engine thrust according to the open loop control policy developed in

Sec. II. To demonstrate the broad concepts of fatigue damage mitigation, the nominal plant model was used in these simulation experiments with exact initial conditions and no disturbances and noise. However, if these conditions are not met, additional feedback control will be necessary because the open loop control alone would be inadequate as discussed in Sec. II. Following the structure in Eq. (6), the cost functional J for nonlinear programming was selected to generate the open loop control policy as

$$J = \sum_{k=0}^{N-1} [\bar{x}_{k+1}^{T} Q \bar{x}_{k+1} + S \dot{v}_k + \bar{u}_k^{T} R \bar{u}_k + W(O_2/H_2)_k^2] \quad (15)$$

where the deviations, $\bar{x}_k$ and $\bar{u}_k$, in the plant state vector and the control input vector, respectively, are defined in Eq. (6); N is the number of the discrete control commands covering the period from the initial time to the final time; and the diagonal matrices Q and R serve as relative weights of the state and input variables. In general, the row vector S (with non-negative entries) penalizes the individual components of the (non-negative) damage rate vector $\dot{v}$ such that

$$\sum_{k=0}^{N-1} S \dot{v}_k$$

represents the scalar measure of the total damage accumulation in Eq. (3) during the mission period. If $S > 0$, then the damage accumulation is minimized in addition to optimization of the plant dynamic performance and control effort. Since
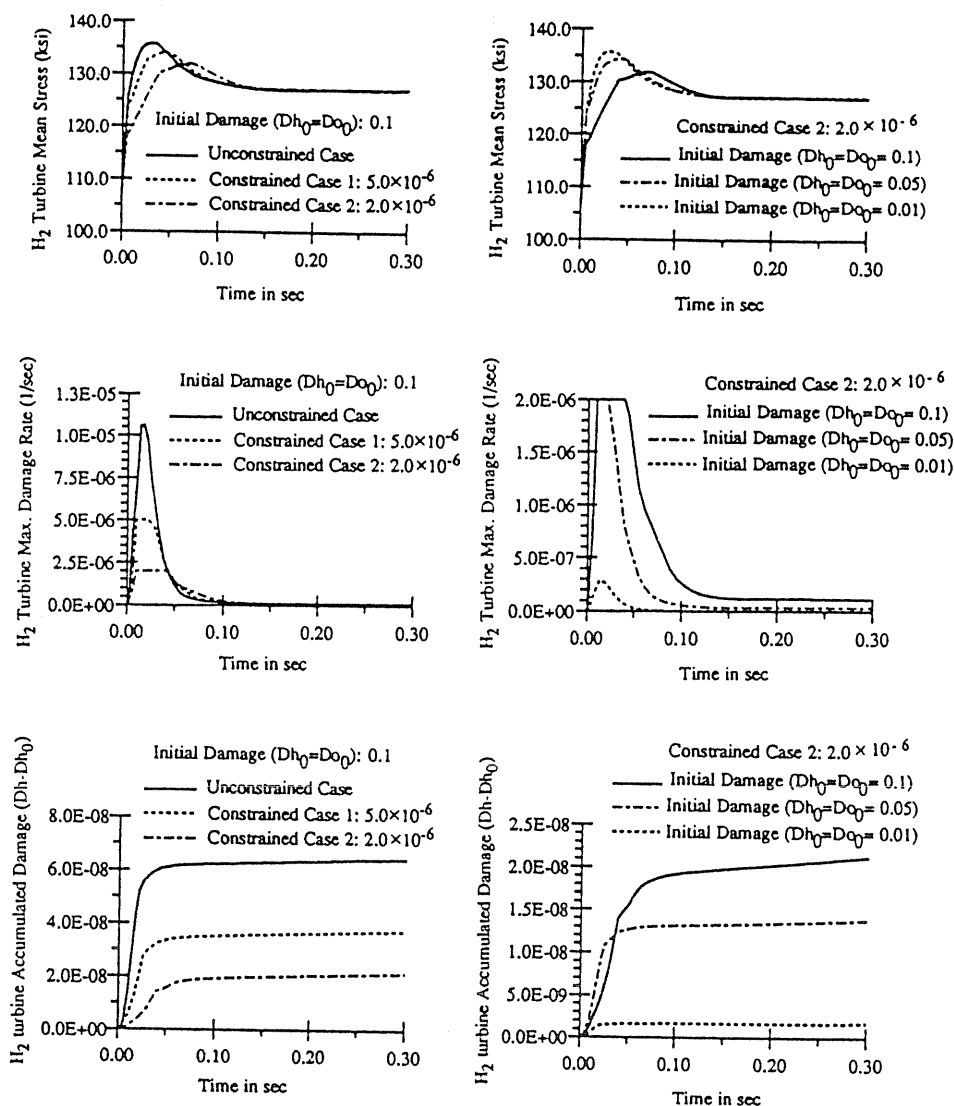
Fig. 6 Transient responses of mean stress, damage rate, and incremental accumulated damage for H_2 turbine.

the rocket engine durability and propellant utilization are very sensitive to the oxidant/fuel (O_2/H_2) ratio, it was brought into the cost functional in Eq. (15) to prevent any large deviations from the desired value of 6.02 through the transients. In the future research, if the main combustion chamber is considered as one of the critical components for damage mitigation, then the explicit dependence of the cost functional on the O_2/H_2 ratio may not be necessary. The simulation results in Figs. 4–7 were obtained with the following relative weights: combustion chamber pressure weight $Q_{55} = 10$, and all other weights $Q_{ii} = 1$, $i \neq 5$; control input weight $R = 0.01I$, where I is the (2×2) identity matrix; and damage rate weight $S = 0$, and O_2/H_2 ratio weight $W = 10$.

The rocket engine model is initiated from an initial equilibrium condition at 2700 psi chamber pressure and O_2/H_2 ratio of 6.02. From this condition, the optimization procedure takes the plant to a new equilibrium position at 3000 psi and the same O_2/H_2 ratio of 6.02 in 300 ms. The control commands to the two oxidant valves are updated at 37 discrete time intervals. That is, N is set equal to 37 in Eq. (15) with nonuniform time intervals between the consecutive instants of step changes in the control command u_k. This sequence of discrete instants was selected based on the results of extensive optimization runs under different choices of N with both uniform and nonuniform spacing. The rationale for using the nonuniform spacing of time in this work is to reduce the size of the optimization problem in the nonlinear programming

procedure by capturing the fast transients during the earlier part of the transient response. The performance cost to be minimized is based on the deviations from the final equilibrium condition at 3000 psi. The results of simulation experiments for the two following conditions are presented as series of curves in the plates of Figs. 4–7.

Simulation condition 1: (The plates on the left side of Figs. 4–7): The respective initial damages for the H_2 turbine and O_2 turbine blades were set to $Dh_0 = 0.1$ and $Do_0 = 0.1$ to represent a used rocket engine. For the unconstrained case and two constrained cases, the damage rates were constrained as listed in Table 2.

Simulation condition 2: (the plates on the right side of Figs. 4–7): To examine the effects of nonlinear damage accumulation, simulation results were generated under three different initial values of the accumulated damage where both Dh_0 and Do_0 were set to 0.01, 0.05, and 0.1, while the damage rate constraints were set identical to that of the constrained case 1 in Table 2.

The transient responses in Figs. 4–7 examine the various engine variables under the above two simulation conditions. The plate in Fig. 4 shows the transient responses of the oxidant flow rates into the O_2 preburner, H_2 preburner, and the main combustor resulting from the optimization over the time frame of 0–300 ms where the control action is updated at the 37 nonuniformly spaced discrete instants of time. The overall system response tends to become more sluggish as the damage
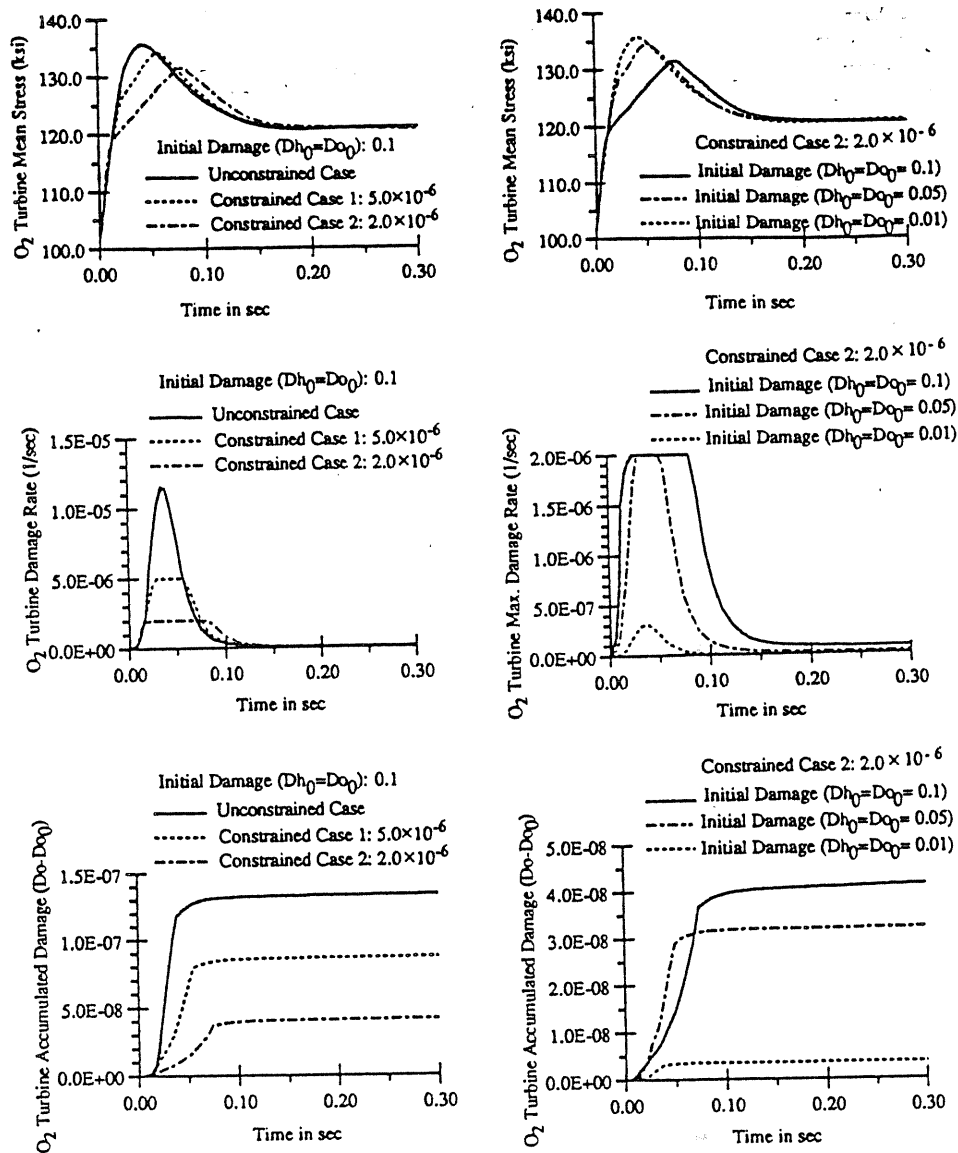
Fig. 7   Transient responses of mean stress, damage rate, and incremental accumulated damage for O_2 turbine.

Table 2   Damage rate constraints $\beta(t)$ for the two cases under simulation condition 1

Time	Constrained case 1	Constrained case 2
0–100 ms	$5.0 \times 10^{-6} \, s^{-1}$	$2.0 \times 10^{-6} \, s^{-1}$
100–200 ms	$1.0 \times 10^{-6} \, s^{-1}$	$1.0 \times 10^{-6} \, s^{-1}$
200–300 ms	$0.5 \times 10^{-6} \, s^{-1}$	$0.5 \times 10^{-6} \, s^{-1}$

rate constraint is made stronger. Similar effects are observed when the initial damage is increased. The rationale for this behavior is that, for a given stress amplitude, the damage rate increases with an increase in the initial damage. This dependence on the initial damage results from the γ parameter in the nonlinear damage model (see Sec. III.B.), and does not occur in the linear damage model where γ is equal to 1. It is important to note that γ is greater than 1 for the high-strength material used in this study. However, for ductile materials such as copper-base alloys used in the thrust chamber cooling tubes, γ may be less than 1, and therefore, the dependence of the control commands on the initial damage should be investigated for the given material under specified operating conditions.

Figure 5 exhibits the effects of the varying oxygen inlet flow into the preburner and the main combustor on the engine dynamics. The resulting transients of the key process varia-

bles, namely, O_2/H_2 ratio, and the gas pressure and temperature in the main combustion chamber, are shown for the two simulation conditions. As expected, for a given level of initial damage, both pressure and temperature dynamics tend to be slower as the constraint is made more severe. Similar effects are seen by increasing the initial values, Do_0 and Dh_0, of the accumulated damage in the O_2 and H_2 turbine blades. The combustor pressure is seen to rise monotonically in all cases after a small dip at about 10 ms, while the preburner pressure (not shown in the figures) keeps on increasing. These plots are largely similar except for the initial transients. Virtually all of fatigue damage accumulation in this transient operation takes place during this short interval (about 0–70 ms) as seen in Figs. 6 and 7. Furthermore, the net excursion of the O_2/H_2 ratio is in the range of 5.8–6.4 in all cases for the up-thrust transient of the rocket engine. The peak value 6.4 of the mixture ratio is about the limit that would be tolerated during a transient excursion. The overshoot in the mixture ratio occurs at about 10 ms when the H_2 turbopump demands more torque to increase its speed so that the pump pressure can be elevated to meet a larger demand of hydrogen flow for the desired mixture ratio. This results in a peak overshoot in the mean stress in the H_2 turbine blades as shown in Fig. 6. Since the turbine blades are the critical components for damage analysis in this study, the pressure ratio across the turbine, which directly influences the torque, is very important. For

a given preburner pressure, a reduction in the combustor pressure causes an increase in the turbine torque. It is the turbine torque and speed that set the cyclic stress and fatigue damage on the turbine blades. Therefore, the dip in the combustor pressure at about 10 ms is also responsible for the peak mean stress in the H_2 turbine blades. Both the mean stress and stress amplitude are the basic inputs to the damage model. The sharp increase in stress is the cause of enhanced damage in the H_2 turbine blades. On the other hand, the peak stress in the O_2 turbine blades occur at about 50 ms as seen in Fig. 7. At this point, the O_2/H_2 ratio has reached its minimum as seen in Fig. 5, and the O_2 turbopump demands more torque to increase its speed so that the pump pressure can be elevated to generate a higher value of oxygen flow for the desired mixture ratio.

The graphs in Figs. 6 and 7 compare the damage rate and the accumulated damage for the two simulation conditions along with the transient responses of the mean stress. For the unconstrained case, the peak stress causes the largest overshoot in the damage rate for both O_2 and H_2 turbine blades. In contrast, for the initial damage of 0.01, the damage rate is within the limit of the constraint even though the peak of mean stress is the largest. This phenomenon is a result of a relatively small slope of the damage curve at the initial stages of the fatigue life. The accumulated damage is seen to be significantly influenced by the constraints and also by the initial damage. This suggests that, for reusable rocket engines, the constraints are best specified based on the knowledge of the initial damage. The damage rate is dependent on the two sequences of control commands, and the oxidant flows into the O_2 and H_2 preburners are changed in response. Therefore, if the initial damage cannot be accurately assessed, then it is conservative to generate the control command sequences on the assumption of a larger value of the initial damage at the expense of the engine performance.

The important observation in these simulation experiments is the substantial reduction in the accumulated damage, which extends the service lives of both O_2 and H_2 turbopumps. The accumulated damage in the unconstrained case is seen to be about three times that of the constrained case. This is a clear message that the consideration of damage in the control of transients to which a rocket engine is exposed can have a considerable impact on the life of critical components (in this case, the turbine blades). It is noted that there is practically insignificant penalty in the response times of the chamber pressure, i.e., the engine thrust, between the unconstrained and the constrained cases. If one is willing to pay a small price in response time, much larger gains on damage reduction can be achieved.

Figures 4–7 exemplify the effects of upthrust transients during a short period of 300 ms. Complete operations of a rocket engine over its life include many thrust transients, and the steady-state operation may last for several hundreds of seconds. Although the damage rate during the steady state is much smaller than that during a transient operation, the total damage accumulation during the steady state may not be relatively insignificant. Therefore, during one flight of a (reusable) rocket engine, the cumulative effects of both transient and steady-state operations need to be considered for estimation of total accumulated damage.

The simulation experiments, described above, only consider a single point of critical stress in each of O_2 and H_2 turbopumps, namely, the turbine blades. In this case, the damage vector is two-dimensional. Simultaneous control of damage at several other critical areas in the rocket engine, such as different locations within the hot sections of the turbines, injector tubes leading to the combustion chamber, and the coolant linings of the combustion chamber and nozzle, shall render the damage vector to be multidimensional. The optimization problem is then to generate control sequences that will not only make a tradeoff between the performance and damage, but also strike a balance between potentially conflicting requirements of damage mitigation at the individual critical points. Although this will make the optimization problem more complex, there is no conceptual difficulty in generating the control sequence for damage mitigation.

V. Summary and Conclusions

The theme of the research in damage-mitigating control of reusable bipropellant rocket engines as reported in this paper is stated as follows:

1) High performance is achieved without overstraining the mechanical structures such that the functional life of critical components is increased resulting in enhanced safety, operational reliability, and availability.

2) For control of complex mechanical systems, damage prediction and damage mitigation are carried out based on the available sensory and operational information such that the plant (i.e., the rocket engine) can be inexpensively maintained, and safely and efficiently driven under diverse operating conditions.

This ongoing research in damage-mitigating control is interdisciplinary involving the fields of active control technology and structural integrity, and is applied to fatigue life prediction and performance optimization in particular. Efficacy of the proposed damage mitigation concept is evaluated for life extension of the turbine blades of a bipropellant rocket engine via simulation experiments. The simulation results suggest that it is possible to enhance the structural durability of reusable rocket engines under transient operations by appropriate maneuvering of the oxidant flow control valves. The damage accumulation in the critical engine components can also be reduced under steady-state operations.

Extended life coupled with enhanced safety and high performance will have a significant economic impact in diverse industrial applications. Furthermore, as the science and technology of materials evolve, the damage characteristics of the structural components can be incorporated within the framework of the proposed damage-mitigating control system.

Applications of damage-mitigating control of power systems include a wide range of engineering applications besides reusable rocket engines for space propulsion. Examples are rotating and fixed wing aircraft, electric power generation plants, automotive and truck engine/transmission systems, and large rolling mills. In each of these systems, damage-mitigating control can enhance safety and productivity accompanied by reduced life cycle cost. A continuous-time damage model will allow timely warnings of these failures and improve maintainability. If the control system is structured with the capability of predicting the impending failures, and thereby exercising authority over the lower level control modules, then the resulting actions would substantially eliminate early shutdown and other disruptions in plant operations with relatively insignificant reduction in plant performance. A more complex application of the damage mitigation concept is the startup and scheduled shutdown of rocket engines and powerplants, and takeoff and landing of aircraft, in which the damage information can be utilized for real-time plant control either in the fully automated mode or with human operator(s) in the loop. Another example is the control of automotive engine and transmission systems to reduce stresses in the drive-train components without compromising driving performance and comfort. The result will be a combination of extended life and reduced drive-train mass with associated savings in the fuel consumption.

D. A. Koss of Pennsylvania State University, University Park, Pennsylvania.

References

[1]Lorenzo, C. F., and Merrill, W. C., "Life Extending Control: A Concept Paper," *American Control Conference*, Boston, MA, June 1991, pp. 1080–1095.

[2]Ray, A., Wu, M.-K., Carpino, M., and Lorenzo, C. F., "Damage-Mitigating Control of Mechanical Systems: Part I—Conceptual Development and Model Formulation," *American Control Conference*, San Francisco, CA, June 1993; an expanded version to appear in *Journal of Dynamic Systems, Measurement, and Control.*

[3]Ray, A., Wu, M.-K., Carpino, M., and Lorenzo, C. F., "Damage-Mitigating Control of Mechanical Systems: Part II—Formulation of an Optimal Policy and Simulation," *American Control Conference*, June 1993; an expanded version to appear in *Journal of Dynamic Systems, Measurement, and Control.*

[4]Noll, T., Austin, E., Donley, S., Graham, G., Harris, T., Kaynes, I., Lee, B., and Sparrow, J., "Impact of Active Controls Technology on Structural Integrity," *Proceedings of the AIAA/ASME/ASCE/AHS/ASC 32nd Structures, Structural Dynamics, and Materials Conference*, AIAA, Washington, DC, April 1991, pp. 1869–1878.

[5]Lorenzo, C. F., and Merrill, W. C., "An Intelligent Control System for Rocket Engines: Need, Vision, and Issues," *Control Systems Magazine*, Vol. 12, No. 1, 1991, pp. 42–46.

[6]Vidyasagar, M., *Nonlinear Systems Analysis*, 2nd ed., Prentice Hall, Englewood Cliffs, NJ, 1992.

[7]Sobczyk, K., and Spencer, B. F., Jr., *Random Fatigue: Data to Theory*, Academic Press, Boston, MA, 1992.

[8]Luenberger, D. G., *Linear and Nonlinear Programming*, Addison-Wesley, Menlo Park, CA, 1984.

[9]Wu, M.-K., "Damage-Mitigating Control of Mechanical Systems," Ph.D. Dissertation in Mechanical Engineering, Pennsylvania State Univ., University Park, PA, May 1993.

[10]Bryan, H. H., and Ahuja, K. K., "Review of Crack Propagation Under Unsteady Loading," *AIAA Journal*, Vol. 31, No. 6, 1993, pp. 1077–1089.

[11]Newman, J. C., Jr., "A Crack Closure Model for Predicting Fatigue Crack Growth Under Aircraft Spectrum Loading," *Methods and Models for Predicting Fatigue Crack Growth Under Random Loading*, American Society for Testing and Materials STP 748, 1981, pp. 53–84.

[12]Tucker, L., and Bussa, S., "The SAE Cumulative Fatigue Damage Test Program," *Fatigue Under Complex Loading: Analyses and Experiments*, Vol. AE-6, 1977, pp. 1–54.

[13]Bolotin, V. V., *Prediction of Service Life for Machines and Structures*, ASME Press, New York, 1989.

[14]Wheeler, O. E., "Spectrum Loading and Crack Growth," *Journal of Basic Engineering, Transactions of the American Society of Mechanical Engineering*, Vol. 94, 1972, pp. 181–186.

[15]Bannantine, J. A., Comer, J. J., and Handrock, J. L., *Fundamentals of Metal Fatigue Analysis*, Prentice Hall, Englewood Cliffs, NJ, 1990.

[16]Dowling, N. E., "Fatigue Life Prediction for Complex Load Versus Time Histories," *Journal of Engineering Materials and Technology*, Vol. 105, July 1983, pp. 206–214.

[17]Marco, S. M., and Starkey, W. L., "A Concept of Fatigue Damage," *Transactions of the American Society of Mechanical Engineering*, Vol. 76, No. 4, 1954, pp. 627–632.

[18]Manson, S. S., and Halford, G. R., "Practical Implementation of the Double Linear Damage Rule and Damage Curve Approach for Treating Cumulative Fatigue Damage," *International Journal of Fracture*, Vol. 17, No. 2, 1981, pp. 169–192.

[19]Paris, P. C., and Erdogan, F., "A Critical Analysis of Crack Propagation Laws," *Journal of Basic Engineering, Transactions of the American Society of Mechanical Engineering*, Vol. D85, 1963, pp. 528–534.

[20]Swain, M. H., Everett, R. A., Newman, J. C., Jr., and Phillips, E. P., "The Growth of Short Cracks in 4340 Steel and Aluminum-Lithium 2090," *AGARD Report*, 767, 1990, pp. 7.1–7.30.

[21]Troudet, T., and Merrill, W. C., "A Real-Time Neural Net Estimator of Fatigue Life," *Preprints of International Joint Conference of Neural Networks (IJCNN)*, San Diego, CA, July 1990.

[22]Sutton, G. P., *Rocket Propulsion Elements*, Wiley, New York, 1992.

[23]Duyar, A., Eldem, V., Merrill, W. C., and Guo, T.-H., "State Space Representation of the Open-Loop Dynamics of the Space Shuttle Main Engine," *Journal of Dynamic Systems, Measurement, and Control*, Vol. 113, No. 4, 1991, pp. 684–690.